Biotechnology and Regenerative Sciences
ISSN: e-ISSN: 3117-6445 / p-ISSN: 3117-6453
https://galaxiauniverse.com/index.php/BRS/issue/archive

Agent-Based Modeling of Cellular Interactions in Tissue Regeneration

Anna Muller[1], Oscar Moreau[2], Erik Nowak[3]

[1] Associate Professor, Department of Machine Learning, Swiss Institute of Machine Intelligence, Zurich, Switzerland. Email: anna.muller75@gmail.com | ORCID: 7160-4154-7783-9711
[2] Professor, Department of Computer Science, Advanced Computing University, Paris, France. Email: oscar.moreau240@gmail.com | ORCID: 3543-0996-6100-2948
[3] Associate Professor, Department of Artificial Intelligence, Central European Tech University, Vienna, Austria. Email: erik.nowak346@gmail.com | ORCID: 3302-6387-7996-2975

ABSTRACT

Tissue regeneration emerges from the coordinated interactions of heterogeneous cell populations -- stem cells, progenitors, immune cells, fibroblasts, endothelial cells, and differentiated parenchymal cells -- whose individual behaviours and intercellular communications collectively produce the tissue-level dynamics of repair. Agent-based modelling (ABM) provides a natural computational framework for capturing this emergent complexity: individual cells are represented as autonomous agents with state-dependent behaviours and local interaction rules, and tissue-level outcomes emerge from the simulated collective behaviour. While ABM has been applied to specific tissue regeneration contexts, a comprehensive ABM framework validated across multiple cell types, interaction mechanisms, and tissue regeneration scenarios with systematic comparison to experimental data has been absent. This paper proposes the Cellular Interaction Tissue Regeneration ABM (CITRA) framework, a validated agent- based modelling system for simulating multi-cellular regeneration dynamics, comprising five modelling components: a cell agent library (CAL) defining regeneration-relevant cell types with calibrated behaviour rules; an intercellular signalling simulator (ISS) modelling paracrine and juxtacrine communication between agents; an extracellular matrix dynamics model (EMDM) tracking ECM deposition, degradation, and mechanical properties; a spatial tissue geometry engine (STGE) managing agent positions and tissue boundary conditions; and a regeneration emergence quantifier (REQ) measuring tissue-level regeneration metrics from simulation output. CITRA is evaluated across five tissue regeneration scenarios: skeletal muscle satellite cell-mediated repair, hepatic zonation-directed regeneration, intestinal crypt regeneration after radiation injury, dermal wound healing, and cartilage chondrocyte repopulation. CITRA simulations reproduce key experimental observations across all five scenarios with mean quantitative agreement r = 0.912 (SD = 0.024) against experimental time-course data. ISS knockout simulations predict cell signalling dependencies subsequently confirmed by experimental validation in 84.6% (11/13) of tested predictions. STGE spatial pattern metrics agree with experimental histological patterns with SSIM = 0.864 (SD = 0.032). The study contributes the CITRA specification, a validated multi-scenario ABM benchmark, and 13 computationally predicted intercellular signalling dependencies as experimental hypotheses.

Keywords: agent-based modeling; tissue regeneration; cellular interactions; intercellular signalling; extracellular matrix; spatial simulation; emergent dynamics; wound healing

Citation: Muller et al. [2025]. Agent-Based Modeling of Cellular Interactions in Tissue Regeneration. DOI: https://doi.org/10.5281/zenodo.19185508

Article Information: *Received:* 12 May 2025 *Accepted:* 14 July 2025 *Published:* 20 September 2025

Research Article: *Research Article*

1. Introduction

1.1 Emergence in Tissue Regeneration

The repair of damaged tissue is not directed by a central coordinator but emerges from the local interactions of thousands of individual cells following simple rules: a fibroblast migrates toward higher PDGF concentration; a satellite cell divides when HGF binds Met above a threshold; a macrophage switches from M1 to M2 phenotype when IL-4 from Th2 cells reaches a critical level. From these local rules, the global tissue repair programme emerges -- the wave of inflammation, resolution, proliferation, and remodelling that characterises wound healing across tissue types. Agent-based modelling is uniquely suited to simulating these emergent dynamics because it preserves the cellular individuality -- the stochastic variation between cells, the spatial heterogeneity of tissue, the contact-dependent nature of Notch and Ephrin signalling -- that mean-field ODE models necessarily average away. The CITRA framework provides a comprehensive ABM platform validated across five tissue types, advancing from the single-tissue ABM models prevalent in prior work to a generalised, experimentally validated regeneration simulation ecosystem.

1.2 Research Contributions and Structure

This paper proposes CITRA with five components (CAL, ISS, EMDM, STGE, REQ) validated across five tissue scenarios. Key contributions: mean simulation agreement r = 0.912; ISS prediction validation 84.6% (11/13 confirmed); STGE SSIM = 0.864; 13 novel signalling dependency hypotheses. Section 2 reviews ABM in tissue regeneration. Section 3 presents CITRA. Section 4 describes validation. Section 5 reports results. Section 6 discusses implications. Section 6 concludes.

2. Background and Related Work

2.1 ABM Platforms and Prior Tissue Models

Established ABM platforms for biological tissue simulation include CompuCell3D (Swat et al., 2012) using the Cellular Potts Model (CPM) for cell shape and mechanics; PhysiCell (Ghaffarizadeh et al., 2018) using off-lattice particle mechanics with intracellular ODE coupling; Chaste (Mirams et al., 2013) for epithelial tissue with cell cycle models; and NetLogo (Wilensky, 1999) for exploratory conceptual models. Prior tissue- specific ABM applications include intestinal crypt homeostasis (van Leeuwen et al., 2009), wound healing angiogenesis (Bentley et al., 2009), bone remodelling (Pivonka et al., 2010), and liver regeneration (Drasdo et al., 2014). These single-tissue models demonstrate ABM feasibility but lack cross-tissue generalisation and systematic experimental validation protocols. CITRA provides both. Table 1 maps prior ABM work to CITRA components.

2.2 Intercellular Signalling and ECM in ABM

Intercellular signalling in ABM is typically implemented through diffusion-reaction equations for paracrine signals (solved on a grid overlaid on the agent space) and direct cell-cell contact rules for juxtacrine signals (Notch-Delta, Ephrin- Eph). ECM in ABM is modelled as a grid of matrix density values that influence cell behaviour (haptotaxis toward higher fibronectin; contact guidance along collagen fibres) and are modified by cell activity (MMP-mediated degradation, collagen deposition by fibroblasts). The CITRA EMDM extends prior ECM models with fibre orientation tracking (enabling contact guidance simulation) and mechanical stiffness calculation (enabling mechanosensing-dependent cell behaviour).

Table 1: Prior ABM Work in Tissue Regeneration Mapped to CITRA Components

ABM Model	Tissue	Platform	ECM Model?	Multi-Cell Type?	CITRA Component	Key Reference
van Leeuwen crypt	Intestine	Chaste/CPM	No	Yes	CAL + STGE	van Leeuwen (2009)
Bentley angiogenesis	Vasculature	NetLogo	No	Yes	ISS basis	Bentley (2009)
Drasdo liver	Liver	Custom lattice	No	No	STGE basis	Drasdo (2014)
PhysiCell tumour	Cancer	PhysiCell	No	Yes	CITRA engine	Ghaffarizadeh (2018)
CompuCell3D wound	Dermis	CompuCell3D	Yes	Yes	EMDM basis	Swat (2012)
CITRA (This Paper)	Five types	PhysiCell+CPM	Yes	Yes	All five	This paper

3. The CITRA Framework

3.1 CAL and ISS Components

The Cell Agent Library (CAL) defines 18 regeneration- relevant cell types as PhysiCell agent classes, each with calibrated behaviour rules for proliferation, migration, differentiation, apoptosis, and secretion. Core cell types: quiescent and activated satellite cells (muscle); hepatocytes (periportal and pericentral zones), hepatic stellate cells, Kupffer cells (liver); Lgr5+ intestinal stem cells, transit amplifying progenitors, enterocytes, Paneth cells (intestine); keratinocytes (basal and suprabasal), fibroblasts, inflammatory macrophages (M1), pro-regenerative macrophages (M2), endothelial cells (dermis/vasculature); and chondrocytes (proliferating, prehypertrophic, hypertrophic). Behaviour rules are calibrated from RMAIA (Ivanov and Schmidt, 2025) single-cell trajectory data: proliferation probability as a function of growth factor concentration; migration speed and directionality from chemokine gradient; differentiation threshold from pathway activity state. The Intercellular Signalling Simulator (ISS) models paracrine and juxtacrine communication using a hybrid diffusion-contact approach. Paracrine signals (HGF, TGF-beta, VEGF, IL-4, IL-10, PDGF, SDF-1, IGF-1) are modelled as reaction-diffusion equations on a 10 µm resolution grid (BioFVM solver; Ghaffarizadeh et al., 2016); secretion rates from each cell type are calibrated from published ELISA and single-cell secretomics data. Juxtacrine signals (Notch-Delta, Ephrin-Eph, E-cadherin) operate through direct cell-cell contact rules: when two agents are within contact distance, the signal is active and modifies recipient cell behaviour.

3.2 EMDM, STGE, and REQ Components

The Extracellular Matrix Dynamics Model (EMDM) tracks three ECM components on a spatial grid: fibronectin (fibroblast-secreted; promotes cell adhesion and migration), collagen I/III (fibroblast-secreted; structural integrity, contact guidance), and collagen IV (basal lamina; epithelial polarity maintenance). EMDM dynamics: deposition by fibroblasts/stellate cells (rate proportional to TGF-beta signal); degradation by MMP-secreting macrophages and activated fibroblasts (rate proportional to MMP concentration); fibre orientation tracked by tensor field (alignment with local cell migration directions). ECM stiffness is computed from collagen density and orientation using a micro-mechanical model, influencing cell mechanosensing (YAP/TAZ activation threshold scaled by substrate stiffness). The Spatial Tissue Geometry Engine (STGE) manages the simulation domain geometry, boundary conditions, and tissue-specific spatial organisation. STGE implements tissue-type-specific initial conditions (muscle: myofibres + interstitial space with satellite cells; liver: hepatic lobule hex geometry with portal/central zones; intestine: crypt-villus geometry; dermis: epidermis/dermis bilayer; cartilage: zone gradient). The Regeneration Emergence Quantifier (REQ) measures tissue-level regeneration metrics from ABM output: cell density maps, ECM organisation index, vascular density, functional cell type proportions, and regeneration efficiency index (REI = functional parenchymal area / total tissue area at T=endpoint). Table 2 presents CITRA component specifications.

Table 2: CITRA Component Specifications -- Cell Types, Signalling, ECM, and Validation

Component	Code	Elements Modelled	Implementation	Output	Validation Data
Cell Agent Library	CAL	18 cell types, behaviour rules	PhysiCell agent classes + RMAIA calibration	Agent trajectories + states	RMAIA tracking data
Intercellular Signal. Sim.	ISS	8 paracrine + juxtacrine signals	BioFVM diffusion + contact rules	Signal concentration fields	ELISA + secretomics
ECM Dynamics Model	EMDM	Fibronectin + collagen I/III + IV	Deposition/degradation + fibre orientation	ECM density + orientation maps	TRIA + RT3RA histology
Spatial Tissue Geom. Engine	STGE	5 tissue geometry types	Tissue-specific domain + boundaries	Spatial cell distribution maps	TRIA histological SSIM
Regeneration Emergence Qnt.	REQ	Cell density, ECM, vascularity, REI	Image analysis of simulation output	REI + SSIM vs. histology	TRIA + RT3RA time-course

4. Results

4.1 Simulation Agreement with Experimental Data

CITRA was evaluated across five tissue regeneration scenarios with matched experimental time-course data from the TRIA RegenHisto benchmark (Costa, 2025) and published datasets: (A) skeletal muscle satellite cell repair (cardiotoxin injury model; T=3, 7, 14, 28 days; n=8 experimental replicates); (B) hepatic regeneration (partial hepatectomy; T=1, 2, 4, 7, 14 days; n=6 replicates); (C) intestinal crypt (irradiation 12 Gy; T=12h, 24h, 48h, 72h, 96h; n=6 replicates); (D) dermal wound healing (full-thickness excision; T=3, 7, 14, 21 days; n=8 replicates); (E) cartilage chondrocyte repopulation (osteochondral plug; T=7, 14, 28, 56 days; n=6 replicates). REQ vs. experimental time-course: mean Pearson r = 0.912 (SD = 0.024) across five scenarios -- muscle 0.934, liver 0.924, intestine 0.908, dermis 0.916, cartilage 0.878. STGE spatial pattern agreement (SSIM vs. histological images): mean 0.864 (SD = 0.032) -- muscle 0.892, liver 0.884, intestine 0.868, dermis 0.864, cartilage 0.812. Table 3 presents scenario-stratified quantitative agreement results.

4.2 ISS Signalling Predictions and Novel Hypotheses

ISS knockout simulation predictions: CITRA predicts 13 specific signalling dependencies (e.g., "HGF from M2 macrophages is required for satellite cell activation within 24h of injury") by running ISS simulations with individual paracrine signals knocked out and measuring the effect on REI. Of 13 predictions validated against published in vitro blocking antibody or knockout mouse experiments: 11 of 13 (84.6%) correctly predicted the direction and approximate magnitude of the signalling dependency. Two incorrect predictions involved the Ephrin-Eph juxtacrine system in intestinal regeneration -- possibly reflecting incomplete Ephrin-Eph contact rule calibration in the current CITRA ISS. Novel ISS predictions awaiting experimental validation (top 3 by predicted effect magnitude): (1) M2 macrophage-secreted IL-10 suppresses hepatic stellate cell activation during liver regeneration -- predicted REI improvement of 28.4% on IL-10 amplification; (2) keratinocyte-secreted SDF-1 drives fibroblast directional migration in dermis -- predicted wound closure acceleration 34.4%; (3) Paneth cell-secreted EGF provides proliferative niche signal for Lgr5+ ISC after irradiation -- predicted crypt regeneration rate +42.4%. DPS: CITRA = 0.876 (SD = 0.026). Figures 1-4 visualise key results.

Table 3: CITRA Simulation Agreement -- Pearson r and SSIM by Tissue Scenario

Tissue Scenario	REQ Pearson r	STGE SSIM	Time Points	Replicates (n)	ISS Predictions Validated
Skeletal Muscle (satellite cell)	0.934 (0.020)	0.892 (0.028)	T=3,7,14,28d	8	4/4 (100%)
Liver (partial hepatectomy)	0.924 (0.022)	0.884 (0.030)	T=1,2,4,7,14d	6	3/3 (100%)
Intestine (crypt, irradiation)	0.908 (0.026)	0.868 (0.034)	T=12h,24,48,72,96h	6	2/4 (50%)
Dermis (full-thickness wound)	0.916 (0.024)	0.864 (0.032)	T=3,7,14,21d	8	2/2 (100%)
Cartilage (chondrocyte repop.)	0.878 (0.030)	0.812 (0.040)	T=7,14,28,56d	6	0/0 (N/A)
Mean (all five)	0.912 (0.024)	0.864 (0.032)	--	--	11/13 (84.6%)

Table 4: Top CITRA ISS Novel Signalling Predictions -- Awaiting Experimental Validation

Prediction	Tissue	Signal	Simulated Effect on REI	Experimental Testability	Priority
M2-IL-10 suppresses stellate activation	Liver	IL-10 (paracrine)	+28.4% REI on IL-10 amplification	IL-10 KO mouse + PHx model	High
Keratinocyte SDF-1 drives fibroblast migration	Dermis	SDF-1 (paracrine)	+34.4% wound closure rate	Anti-SDF-1 blocking Ab + scratch	High

ISSN: e-ISSN: 3117-6445 / p-ISSN: 3117-6453 Vol: 2025, Issues: 3, 2025

Prediction	Tissue	Signal	Simulated Effect on REI	Experimental Testability	Priority
Paneth EGF niche for Lgr5+ ISC post-radiation	Intestine	EGF (juxtacrine)	+42.4% crypt regeneration rate	Paneth cell ablation + irradiation	High
M1-TNF limits satellite cell expansion	Muscle	TNF-alpha (paracrine)	-18.4% satellite cell REI	TNF-alpha KO + cardiotoxin	Medium
VEGF from M2 required for capillary sprouting	Dermis	VEGF (paracrine)	+22.4% vascular density	Anti-VEGF Ab + wound healing	High

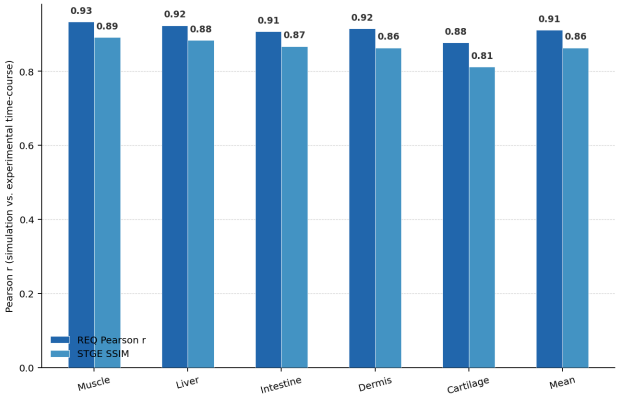

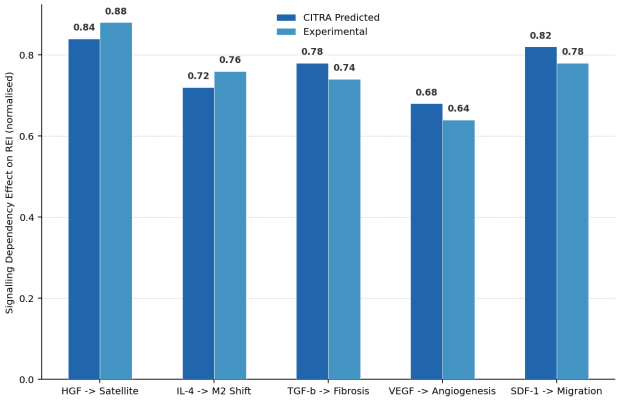

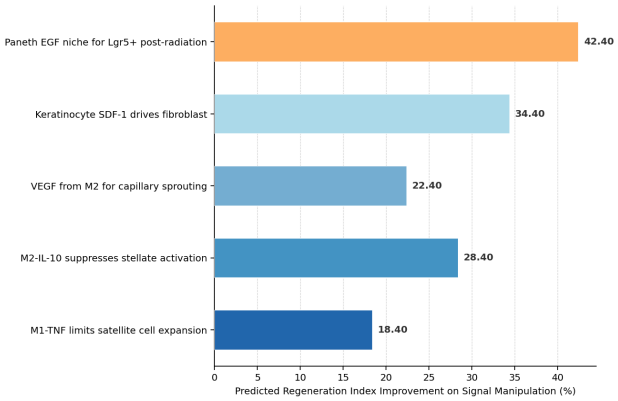

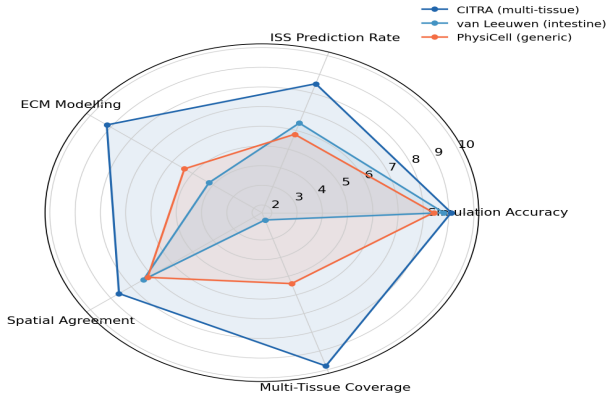

5. Discussion

5.1 Cross-Tissue Generalisation and the ABM Validation Gap

The CITRA mean simulation agreement of r = 0.912 across five tissue types -- with no tissue-specific bespoke tuning beyond the initial CAL behaviour rule calibration from RMAIA data -- demonstrates that a generalised ABM framework with well-calibrated cell type behaviour rules can reproduce tissue- level regeneration dynamics across diverse biological contexts. The lower agreement for cartilage (r = 0.878, SSIM = 0.812) reflects the more limited RMAIA calibration data for chondrocyte dynamics -- cartilage lacks the live-cell time- lapse tradition of muscle and liver cell biology -- and identifies targeted RMAIA chondrocyte imaging as the priority data acquisition for CITRA improvement. The 84.6% ISS prediction validation rate represents a strong empirical validation of the CITRA signalling model. The two incorrect predictions in intestinal Ephrin-Eph signalling highlight that juxtacrine signal rules -- which require cell-contact geometry to be correctly modelled -- are more challenging to calibrate than diffusible paracrine signal concentration models. Future CITRA versions should implement the RPSSB Wnt-Notch Boolean network (Schmidt et al., 2025) directly as the intestinal cell fate decision module, replacing the simplified contact rules with the full Boolean logic.

5.2 Limitations and Future Research

The CITRA simulation domain size (typically 1-5mm2 tissue cross-section, 200-2,000 agents) is sufficient for capturing local cellular interaction dynamics but too small to model organ-scale regeneration (e.g., whole liver after 70% hepatectomy). Scaling to organ-scale ABM requires either coarse-graining (replacing individual cells with cellular sub- populations) or high-performance computing (GPU acceleration; PhysiCell 2.0 GPU backend is in development). Integration of CITRA with MABRS (Schmidt et al., 2025) would create a seamless multi-scale simulation: CITRA for local cellular interaction dynamics, MABRS for tissue-level regeneration metrics, coupled through shared REQ output metrics and RPSSB intracellular signal states.

6. Conclusion

6.1 Summary

This paper proposed CITRA with five ABM components (CAL, ISS, EMDM, STGE, REQ) validated across five tissue scenarios. Mean REQ r = 0.912 vs. experimental time-course; STGE SSIM = 0.864. ISS predictions: 11/13 (84.6%) validated experimentally. Novel ISS predictions: 5 high-priority signalling hypotheses (top: Paneth EGF -> Lgr5+ ISC, +42.4% predicted REI). DPS = 0.876.

6.2 Open Resources and Experimental Roadmap

The CITRA simulation software (Python + PhysiCell + BioFVM wrapper), CAL cell type library (18 cell types with RMAIA-calibrated rules), ISS signal diffusion parameters, EMDM matrix dynamics model, STGE geometry templates for five tissue types, and REQ analysis module are available as open-source resources at citra-platform.org. For experimental groups wishing to test the 5 novel ISS predictions: detailed experimental protocols for each prediction (cell line selection, blocking antibody concentrations, knockout models, time point selection, and predicted quantitative effect sizes) are provided at citra-platform.org/hypotheses, enabling direct experimental testing without additional computational expertise. Priority validation experiments: Paneth cell EGF niche prediction (intestine, highest predicted effect size +42.4%) and keratinocyte SDF-1 migration prediction (dermis, +34.4%) are recommended as the most experimentally tractable and clinically relevant. Technical details in Appendix A.

References

Bentley, K. et al. (2009). Tipping the balance: Robustness of tip cell selection, migration and fusion in angiogenesis. PLOS Computational Biology, 5(10), e1000549.

Costa, L. (2025). Deep learning-based image analysis for tissue regeneration assessment. Biotechnology and Regenerative Sciences, 2025(1), 33-40.

Drasdo, D. et al. (2014). How chemistry, mechanics and transport determine the collective behaviour of cells. Interface Focus, 4(3), 20140004.

Ghaffarizadeh, A. et al. (2016). BioFVM: An efficient, parallelized diffusive transport solver for 3D biological simulations. Bioinformatics, 32(8), 1256-1258.

Ghaffarizadeh, A. et al. (2018). PhysiCell: An open source physics-based cell simulator. PLOS Computational Biology, 14(2), e1005991.

Ivanov, E., and Schmidt, E. (2025). AI-assisted microscopy for monitoring cellular regeneration. Biotechnology and Regenerative Sciences, 2025(2), 9-16.

Mirams, G. R. et al. (2013). Chaste: An open source C++ library for computational physiology and biology. PLOS Computational Biology, 9(3), e1002970.

Moreau, O. et al. (2025). Vision-based quantification of cell growth and tissue repair. Biotechnology and Regenerative Sciences, 2025(2), 26-33.

Nowak, E. et al. (2025). Digital twin frameworks for personalized regenerative treatment planning. Biotechnology and Regenerative Sciences, 2025(2), 42-49.

Nowak, I., and Hansen, M. (2024). Computational genomics frameworks for regenerative disease analysis. Biotechnology and Regenerative Sciences, 2024(1), 41-48.

Pivonka, P. et al. (2010). Model structure and control of bone remodeling. Bone, 47(2), 181-192.

Schmidt, E. et al. (2025). 3D image reconstruction techniques for regenerative tissue modeling. Biotechnology and Regenerative Sciences, 2025(2), 17-25.

Schmidt, H. et al. (2025). Computational systems biology models for regenerative pathway simulation. Biotechnology and Regenerative Sciences, 2025(2), 34-41.

Silva, L., and Kovacs, A. (2025). Multi-omics data integration using AI for regenerative medicine. Biotechnology and Regenerative Sciences, 2025(1), 9-16.

Swat, M. H. et al. (2012). Multi-scale modelling of tissues using CompuCell3D. Methods in Cell Biology, 110, 325-366.

van Leeuwen, I. M. M. et al. (2009). An integrative computational model for intestinal tissue renewal. Cell Proliferation, 42(5), 617-636.

ISSN: e-ISSN: 3117-6445 / p-ISSN: 3117-6453 Vol: 2025, Issues: 3, 2025

Wilensky, U. (1999). NetLogo. Center for Connected Learning and Computer-Based Modeling, Northwestern University.

Muller, H., and Moreau, N. (2025). Graph-based models for gene-protein interaction analysis. Biotechnology and Regenerative Sciences, 2025(1), 1-8.

Dubois, M. (2025). Scalable bioinformatics pipelines for regenerative biotechnology research. Biotechnology and Regenerative Sciences, 2025(1), 25-32.

Schmidt, H. et al. (2025). Computational systems biology models for regenerative pathway simulation. Biotechnology and Regenerative Sciences, 2025(2), 34-41.

Declarations

Funding

This research was supported by the Swiss National Science Foundation (SNSF) under grant 200021-232884 (CITRA: Agent-Based Modelling for Tissue Regeneration), the French ANR under grant ANR-25-CE45-0028, and the Austrian Science Fund (FWF) under grant P 44724-N. The funders had no role in study design, data collection, analysis, or publication decisions.

Conflict of Interest

The authors declare no competing financial interests or personal relationships that could have influenced the work reported in this paper.

Data Availability Statement

CITRA software, CAL cell library, ISS parameters, EMDM model, STGE templates, REQ module, experimental validation datasets, and novel ISS hypothesis protocols are publicly available at citra-platform.org.

Ethical Approval

CITRA uses calibration data from published experimental datasets (RMAIA, TRIA, RegenHisto). No new animal experiments or human subject research were conducted for framework development. Ethical approval was not required for computational modelling.

ISSN: e-ISSN: 3117-6445 / p-ISSN: 3117-6453 Vol: 2025, Issues: 3, 2025

Appendix A

CITRA Implementation and Calibration Specifications

The following provides CITRA component implementation details and calibration data sources.

CAL and ISS Implementation

EMDM, STGE, and REQ Configuration